

# A Complex of Methylthioadenosine/*S*-Adenosylhomocysteine Nucleosidase, Transition State Analogue, and Nucleophilic Water Identified by Mass Spectrometry

Shanzhi Wang,<sup>†</sup> Jihyeon Lim,<sup>‡</sup> Keisha Thomas,<sup>†</sup> Funing Yan,<sup>†</sup> Ruth H. Angeletti,<sup>‡</sup> and Vern L. Schramm<sup>\*†</sup>

<sup>†</sup>Department of Biochemistry, Albert Einstein College of Medicine, 1300 Morris Park Avenue, Bronx, New York 10461, United States

<sup>‡</sup>The Laboratory for Macromolecular Analysis & Proteomics, Albert Einstein College of Medicine, 1300 Morris Park Avenue, Bronx, New York 10461, United States

## S Supporting Information

**ABSTRACT:** An enzyme-stabilized nucleophilic water molecule has been implicated at the transition state of *Escherichia coli* methylthioadenosine nucleosidase (*Ec*MTAN) by transition state analysis and crystallography. We analyzed the *Ec*MTAN mass in complex with a femtomolar transition state analogue to determine whether the inhibitor and nucleophilic water could be detected in the gas phase. *Ec*MTAN–inhibitor and *Ec*MTAN–inhibitor–nucleophilic water complexes were identified by high-resolution mass spectrometry under nondenaturing conditions. The enzyme–inhibitor–water complex is sufficiently stable to exist in the gas phase.

In comparison with solution reactions, enzymes enhance reaction rates by as much as 20 orders of magnitude.<sup>1</sup> Along the reaction coordinate of an enzyme-catalyzed reaction, a transition state is reached by a dynamic search of enzyme–reactant geometry.<sup>2,3</sup> Molecules mimicking the structure of a transition state convert the rare enzymatic geometry of the transition state to a stable complex that binds with high affinity to the targeted enzymes.<sup>4–8</sup> Transition state structures for enzymatic reactions have been established by the combination of kinetic isotope effects and quantum computational calculations.<sup>3,9,10</sup> Using this approach, transition states of 5'-methylthioadenosine/*S*-adenosylhomocysteine nucleosidases (MTANs) from several bacterial species have been established.<sup>11–13</sup> Transition state analogue inhibitors have been designed and synthesized with  $K_i$  values in the femtomolar range.<sup>14</sup> This tight binding is proposed to support faithful mimicry of the transition state structure. Transition state analysis and crystal structures of MTAN with transition state analogue inhibitors have implicated a crystallographic water molecule in a position to act as the nucleophile. Tightly bound inhibitors have low release rates in solution, and we wanted to see whether a transition state analogue together with its nucleophilic water would be retained in the gas phase during mass spectrometry experiments.

MTAN is a dimeric enzyme that catalyzes hydrolytic depurination of 5'-methylthioadenosine (MTA) and *S*-adenosylhomocysteine. The transition state for MTA hydrolysis by *Ec*MTAN has been reported to be a 5-methylthioribocation

and a neutral adenine, with a C1' to N9 distance of 3 Å or more.<sup>11</sup> A nucleophilic water molecule was proposed to be part of the transition state complex (Figure 1). Water attacks C1' of

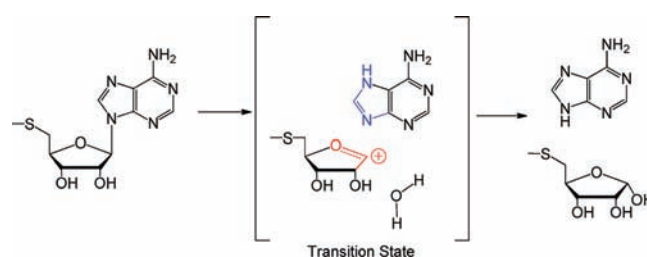


**Figure 1.** Transition state structure of MTA catalyzed by *Ec*MTAN.<sup>13</sup>

the ribocation to complete the reaction.<sup>11</sup> If a transition state lifetime of  $10^{-14}$  s is assumed,<sup>15</sup> the nucleophilic water must be preorganized at the attacking position. The transition state lifetime is too short to permit significant water diffusion.<sup>16</sup> Transition state analogues mimicking the geometry and molecular electrostatic potential of the transition state structure of MTANs have  $K_i$  values in the femtomolar range.<sup>14</sup>

Crystal structures with transition state analogue complexes have revealed an extensive bonding network with the enzyme (Figure 2),<sup>17,18</sup> consistent with the powerful binding interactions. BuT-DADMe-ImMA (Figure 2A) has a high affinity for *Ec*MTAN ( $K_i = 0.3$  pM), and its structure has been solved with *Vibrio cholerae* MTAN (*Vc*MTAN), which shares 60% sequence identity with *Ec*MTAN. The inhibitor is bound in the active site with five favorable hydrogen bonds to the protein, two hydrogen bonds to the nucleophilic water molecule, and multiple hydrophobic interactions (Figure 2B and Figure S1 in the Supporting Information). A highly stabilized nucleophilic water molecule is positioned 2.7 Å from the cationic nitrogen ( $pK_a \approx 9$ ) that mimics the 1'-anomeric carbon of the ribocation transition state (Figure 2).<sup>18</sup> This complex contains all elements of the transition state complex, including the nucleophilic water. High-resolution mass spectrometry was applied to determine whether the complex remains intact following extraction into the gas phase.

**Received:** November 29, 2011

**Published:** January 5, 2012

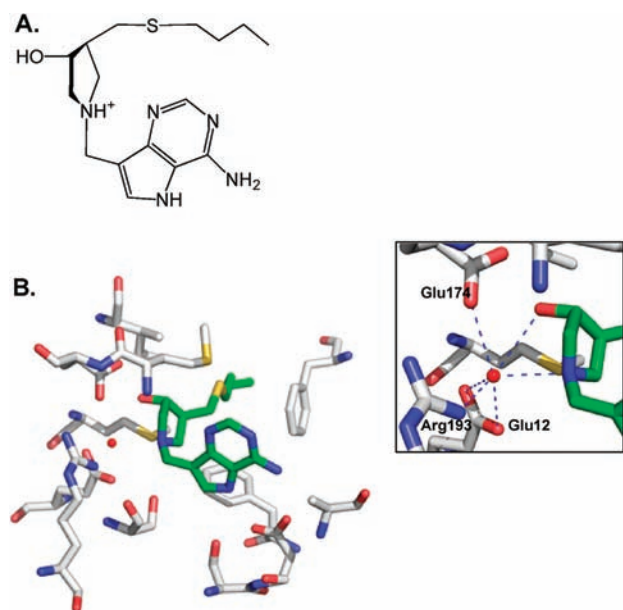


**Figure 2.** Complex of *Ec*MTAN, BuT-DADMe-ImmA, and a water molecule. (A) The chemical structure of BuT-DADMe-ImmA is shown in the orientation corresponding to its position in the crystal structure. (B) In the crystal structure (PDB entry 3DP9), BuT-DADMe-ImmA (green) and a water molecule (red dot) are surrounded by active-site residues (gray). Inset: hydrogen-bonding network involving the water molecule. PYMOL was used to generate the graphs.

*Ec*MTAN is a homodimer with a calculated monomer molecular weight of 26029.7 Da. The experimental mass for the apo enzyme was studied from a denatured sample containing 50% methanol and 0.1% formic acid using a nano-electrospray quadrupole time-of-flight (nanoESI-QToF) mass spectrometer. An experimental mass of 26029.6 Da was acquired, confirming the integrity of the expressed enzyme and the absence of bound water or ions (Figure S2A).

Native dimeric *Ec*MTAN in 5 mM ammonium acetate was analyzed and produced peaks at  $m/z$  4339.3, 4005.6, 3719.5, 3471.7, and 3254.7. When deconvoluted for charge states, these correspond to the multiply protonated dimeric MTAN with charge states of 12+, 13+, 14+, 15+, and 16+, respectively. The deconvoluted spectrum gave an experimental dimer molecular mass of 52059.6 Da, in good agreement with the calculated value of 52059.4 Da. Thus, the denatured monomer and native dimer can be mobilized into the gas phase without additional water, ion, or solute molecules (Figure S2B).

The calculated molecular weight of 336.18 for BuT-DADMe-ImmA was also confirmed by mass spectrometry (MS) (Figure S3). Molar equivalent amounts of BuT-DADMe-ImmA and *Ec*MTAN were mixed, and the MS spectrum was acquired under the conditions optimized for dimeric *Ec*MTAN. Peaks generated from this complex were shifted to higher  $m/z$  values than those of dimeric *Ec*MTAN alone (Figure 3). Spectral deconvolution revealed a species at 52730.8 Da corresponding to two inhibitor molecules bound to dimeric *Ec*MTAN. Another peak corresponded to dimer, two inhibitors, and two water molecules, giving a mass peak at 52766.4 Da. Other peaks consistent with addition of Na<sup>+</sup> and/or K<sup>+</sup> ions to the complex were also observed (Figure 3).

An altered protein mass in MS analysis might possibly originate from oxidation of the protein or the inhibitor during

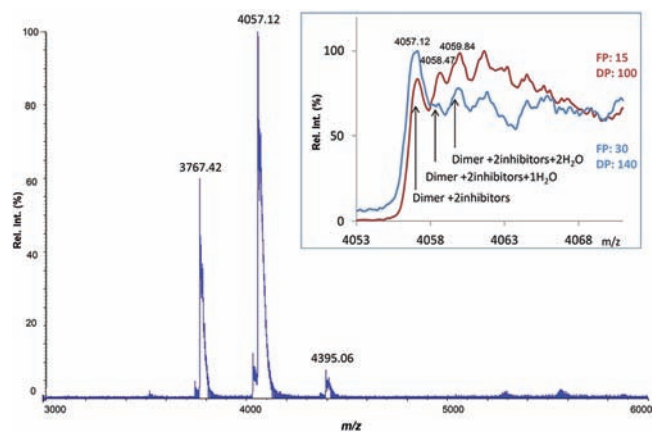


**Figure 3.** MS analysis of *Ec*MTAN in complex with stoichiometric BuT-DADMe-ImmA. Inset: with increased focusing potential and declustering potential, water molecules shift out of the enzyme-inhibitor complex.

high-voltage electrospray. Oxidation would produce a mass shift of 32 Da (addition of two O atoms), in contrast to a shift of 36 Da generated by addition of two water molecules. As indicated above and in the Supporting Information, no oxidation was observed in either apo-MTAN or the inhibitor under our experimental conditions (Figures S2 and S3). Hence, oxidation of the complex of dimeric enzyme and inhibitors was considered unlikely.

Additional tests for the nature of the *Ec*MTAN complexes in MS analysis involved different experimental conditions. During MS analysis, ions are generated, desolvated, and accelerated by potential voltage differences. This is achieved by applying different voltages to components between the ESI tip and the detector. Higher potential accelerates ions faster and results in more energetic collisions with nitrogen along the ion path.<sup>19,20</sup> More energetic collisions would be expected to result in the dissociation of noncovalently bound molecules such as water or inhibitor in the complex.

Different combinations of focusing potential (FP) and declustering potential (DP) generated by differential voltage application were used to produce different potential MS energies. First, mass spectra of the inhibitor-bound complex were acquired with FP = 100 and DP = 15 (in arbitrary potential voltage units) (Figure 3 inset, red). Then, a higher potential was applied (FP = 140 and DP = 30) to investigate possible changes (Figure 3 inset, blue). Mass differences for the three peaks arising from oxidation would not change the peak intensity ratios. However, the high-potential combination increased the peak intensity at  $m/z$  4057.1 relative to the original conditions (Figure 3 inset). The increased intensity of the peak at  $m/z$  4057.1 implies that more energetic collisions under higher-potential conditions caused the loss of water molecules. The apo enzyme produced a single peak at each charge, regardless of changes in the potential. These results support the presence of bound water molecules only in the complex of *Ec*MTAN together with the transition state analogue in the gas phase, and not to the apo enzyme.

Detection of the water molecule agrees with the chemical mechanism of *Ec*MTAN (Figure 1), in which a nucleophilic water attacks C1' at the transition state. Because of the short lifetime of enzymatic transition states ( $<10^{-14}$  s),<sup>15</sup> the water molecule must be preorganized near C1' at the transition state. During the transition state lifetime, there is insufficient time for

water diffusion. This preorganization explains the affinity of bound water in complex with the transition state analogue. The crystal structure shows the presumptive water molecule hydrogen-bonded with the 3'-OH and N1' of BuT-DADMe-ImmA as well as the side chains of Arg193, Glu12, and Glu174 of MTAN (Figure 2). Consequently, we propose that the water molecules identified by MS are the nucleophilic waters.

We did not observe the *Ec*MTAN dimer bound to only one inhibitor unless we intentionally formed this complex by substoichiometric inhibitor titration (Figure S4). Thus, the inhibitor binds to both subunits with sufficient affinity to be retained in the gas phase. The stoichiometric binding of the inhibitor with *Ec*MTAN results from the low dissociation rate constant ( $k_{\text{off}}$ ). In solution, the association rate constant ( $k_{\text{on}}$ ) and slow-onset conformational change for inhibitors that bind tightly to MTAN is on the order of  $10^3 \text{ s}^{-1}$ . To achieve a  $K_{\text{i}}$  value in the femtomolar range,  $k_{\text{off}}$  should be on the order of  $10^{-9} \text{ s}^{-1}$ . Consistent with this approximation of  $k_{\text{off}}$  incubation of the enzyme–inhibitor complex in solution with a near-saturation concentration of MTA (2 mM) did not restore significant enzymatic activity in a 3 h incubation.

BuT-DADMe-ImmA has a  $K_{\text{i}}$  value of 0.3 pM with *Ec*MTAN and binds to the enzyme with a geometry similar to that of the substrate.<sup>21</sup> Both inhibitor and enzyme contacts are needed to bind the nucleophilic water molecule in the enzyme. The numbers of favorable hydrogen bonds and hydrophobic interactions increase when a substrate analogue of MTA is replaced with BuT-DADMe-ImmA at the catalytic site.<sup>21,22</sup> In addition, a new ionic interaction is formed between the inhibitor cation and the immobilized nucleophilic water.<sup>18,22</sup> Thus, BuT-DADMe-ImmA is an excellent transition state analogue with high binding affinity to *Ec*MTAN and an ability to stabilize the nucleophilic water molecule. A second crystallographic water in contact with the nucleophilic water is weakly bound with only one favorable hydrogen bond (Figure S1).

Although BuT-DADMe-ImmA and *Ec*MTAN function to stabilize a catalytic-site water, the water molecule has a weaker affinity to the protein than the inhibitor. Complexes were detected by MS with substoichiometric amounts of water, reflecting the dynamic hydrogen-bonding nature of water and its weaker hydrogen-bonding network. Supersaturation with inhibitor produced two additional smaller peaks at  $m/z$  4085.7 and 4111.5 (Figure S5), corresponding to enzyme complexes with one and two additional inhibitors bound per dimer, respectively, but with no additional water molecules. These peaks are attributed to nonspecific binding of the inhibitor (acting as a cation) and the enzyme.

An attempt to measure the exchange rate of  $\text{H}_2^{16}\text{O}$  from the enzyme–inhibitor–water complex used dilution experiments into  $\text{H}_2^{18}\text{O}$  followed by MS analysis. However, the expected mass change could not be reliably distinguished from the enzyme dimer +  $\text{K}^+$  mass under our experimental conditions.

Along the reaction coordinate of *Ec*MTAN, a fully dissociated ribocation transition state is formed. Sugar cations are highly reactive and susceptible to attack by any nearby nucleophile.<sup>16</sup> Thus, enzymes forming sugar cation transition states must stabilize the attacking group within electron-reorganization distance of the reaction center. The related enzyme purine nucleoside phosphorylase immobilizes a phosphate nucleophile for reaction of the phosphate with the ribocation, and motion along the reaction coordinate involves altered ribose sugar pucker that occurs on the time scale of 70

fs, the reaction coordinate lifetime, of which 10 fs is the lifetime of the ribocation transition state.<sup>15</sup> For a transition state analogue to mimic the transition state, it is required to mimic the ribocationic feature of the transition state and also to stabilize the attacking nucleophile. Using MS under non-denaturing conditions at neutral pH, we were able to identify the presumptive nucleophilic water molecule in complex with the transition state analogue BuT-DADMe-ImmA and *Ec*MTAN. The results support the proposed chemical mechanism and demonstrate the utility of high-resolution MS to detect interesting noncovalent complexes formed along the reaction coordinate.

## ■ ASSOCIATED CONTENT

### 📄 Supporting Information

Experimental procedures and Figures S1–S5. This material is available free of charge via the Internet at <http://pubs.acs.org>.

## ■ AUTHOR INFORMATION

### Corresponding Author

vern.schramm@einstein.yu.edu

## ■ ACKNOWLEDGMENTS

We thank Drs. P.C. Tyler and G.B. Evans of Industrial Research Laboratory, Inc. for providing BuT-DADMe-ImmA. This work was financially supported by NIH Grant GM41916.

## ■ REFERENCES

- (1) Radzicka, A.; Wolfenden, R. *Science* **1995**, *267*, 90–93.
- (2) Schramm, V. L. *Arch. Biochem. Biophys.* **2005**, *433*, 13–26.
- (3) Schramm, V. L. *Annu. Rev. Biochem.* **2011**, *80*, 703–732.
- (4) Pauling, L. *Am. Sci.* **1948**, *36*, 51–58.
- (5) Wolfenden, R. *Nature* **1969**, *223*, 704–705.
- (6) Wolfenden, R. *Biophys. Chem.* **2003**, *105*, 559–572.
- (7) Wolfenden, R.; Snider, M. J. *Acc. Chem. Res.* **2001**, *34*, 938–945.
- (8) Schramm, V. L. *J. Biol. Chem.* **2007**, *282*, 28297–28300.
- (9) Schramm, V. L.; Horenstein, B. A.; Kline, P. C. *J. Biol. Chem.* **1994**, *269*, 18259–18262.
- (10) Cleland, W. W. *Arch. Biochem. Biophys.* **2005**, *433*, 2–12.
- (11) Singh, V.; Lee, J. E.; Nunez, S.; Howell, P. L.; Schramm, V. L. *Biochemistry* **2005**, *44*, 11647–11659.
- (12) Singh, V.; Schramm, V. L. *J. Am. Chem. Soc.* **2007**, *129*, 2783–2795.
- (13) Singh, V.; Luo, M.; Brown, R. L.; Norris, G. E.; Schramm, V. L. *J. Am. Chem. Soc.* **2007**, *129*, 13831–13833.
- (14) Gutierrez, J. A.; Luo, M.; Singh, V.; Li, L.; Brown, R. L.; Norris, G. E.; Evans, G. B.; Furneaux, R. H.; Tyler, P. C.; Painter, G. F.; Lenz, D. H.; Schramm, V. L. *ACS Chem. Biol.* **2007**, *2*, 725–734.
- (15) Saen-Oon, S.; Quaytman-Machleder, S.; Schramm, V. L.; Schwartz, S. D. *Proc. Natl. Acad. Sci. U.S.A.* **2008**, *105*, 16543–16548.
- (16) Ghanem, M.; Murkin, A. S.; Schramm, V. L. *Chem. Biol.* **2009**, *16*, 971–979.
- (17) Singh, V.; Shi, W.; Evans, G. B.; Tyler, P. C.; Furneaux, R. H.; Almo, S. C.; Schramm, V. L. *Biochemistry* **2004**, *43*, 9–18.
- (18) Gutierrez, J. A.; Crowder, T.; Rinaldo-Matthis, A.; Ho, M. C.; Almo, S. C.; Schramm, V. L. *Nat. Chem. Biol.* **2009**, *5*, 251–257.
- (19) Sobott, F.; Hernandez, H.; McCammon, M. G.; Tito, M. A.; Robinson, C. V. *Anal. Chem.* **2002**, *74*, 1402–1407.
- (20) Gabelica, V.; De Pauw, E. *Mass Spectrom. Rev.* **2005**, *24*, 566–587.
- (21) Lee, J. E.; Smith, G. D.; Horvatin, C.; Huang, D. J.; Cornell, K. A.; Riscoe, M. K.; Howell, P. L. *J. Mol. Biol.* **2005**, *352*, 559–574.
- (22) Lee, J. E.; Singh, V.; Evans, G. B.; Tyler, P. C.; Furneaux, R. H.; Cornell, K. A.; Riscoe, M. K.; Schramm, V. L.; Howell, P. L. *J. Biol. Chem.* **2005**, *280*, 18274–18282.